Remote Sensing of Environment 139 (2013) 277–290

Contents lists available at ScienceDirect

Remote Sensing of Environment

journal homepage: www.elsevier.com/locate/rse

Monitoring coniferous forest biomass change using a Landsat trajectory-based approach

Magdalena Main-Knorn [a,*], Warren B. Cohen [b], Robert E. Kennedy [c], Wojciech Grodzki [d], Dirk Pflugmacher [a], Patrick Griffiths [a], Patrick Hostert [a]

[a] Geography Department, Humboldt-Universität zu Berlin, Unter den Linden 6, 10099 Berlin, Germany
[b] US Forest Service, Pacific NW Research Station, Corvallis, OR 97331, USA
[c] Department of Earth and Environment, Boston University, 675 Commonwealth Ave., Boston, MA 02215, USA
[d] Forest Research Institute, ul. Fredry 39, 30-605 Krakow, Poland

ARTICLE INFO

Article history:
Received 18 January 2013
Received in revised form 5 August 2013
Accepted 6 August 2013
Available online 6 September 2013

Keywords:
Remote sensing
Landsat time series
SPOT
IRS LISS
LandTrendr
Biomass trajectories
Coniferous
Carpathian Mountains

ABSTRACT

Forest biomass is a major store of carbon and thus plays an important role in the regional and global carbon cycle. Accurate forest carbon sequestration assessment requires estimation of both forest biomass and forest biomass dynamics over time. Forest dynamics are characterized by disturbances and recovery, key processes affecting site productivity and the forest carbon cycle. Thus, spatially and temporally explicit knowledge of these processes and their drivers are critical for understanding regional carbon cycles. Here, we present a new method that uses satellite data to estimate changes in forest aboveground biomass associated with forest disturbances and recovery at annual time steps. First, yearly maps of aboveground biomass between 1985 and 2010 based on Landsat time series and field data were created. Then, we applied a trajectory-based segmentation and fitting algorithm to the yearly biomass maps to reconstruct the forest disturbance and recovery history over the last 25 years.

We tested the method over a coniferous forest region in the Western Carpathian Mountains, which experienced long-term environmental changes. Overall, 55% (~30,700 ha) of the total coniferous forest experienced a loss of biomass over the observation period, while ~30% showed severe or complete removal of forest biomass. At the same time, 11.2% of the area was reforested or regenerated on previously damaged forest stands. The total coniferous biomass dropped by 15% between 1985 and 2010, indicating negative balance between the losses and the gains. Disturbance hotspots indicate high insect infestation levels in many areas and reveal strong interactions between biomass loss and climate conditions. Our study demonstrates how spatial and temporal estimates of biomass help to understand regional forest dynamics and derive degradation trends in regard to regional climate change.
© 2013 Elsevier Inc. All rights reserved.

1. Introduction

Forests store large amounts of carbon and play an important role in the regional and global carbon cycle. Accurate estimates of forest biomass dynamics require accounting for the spatial effects of disturbances and recovery, both affecting forest carbon emissions. The spatial extent and the magnitude of disturbance and regrowth determine the net carbon flux of a forest and the magnitude of carbon loss during and after disturbance (Frolking et al., 2009; Luyssaert Luyssaert et al., 2010). Disturbances can convert forests from a net carbon sink to a net carbon source (during and after the disturbance occurred) (Kurz, Dymond, et al., 2008; Kurz, Stinson, Rampley, Dymond and Neilson, 2008). Because productivity varies considerably by ecoregion and forest type, accurately estimating the mass of living forest material and its changes is critical especially for regional scale carbon models (Kimball, Keyser, Running, & Saatchi, 2000; Schroeder, Gray, Harmon, Wallin, & Cohen, 2008). Remote sensing data and their derivatives provide unique and appropriate input information to assess changes in forest biomass across different spatial and temporal scales (Mickler, Earnhardt, & Moore, 2002; Powell et al., 2010). Here we present a method to estimate and monitor aboveground forest biomass changes with near-annual time-series data.

Forest disturbance and recovery are key processes in forest ecosystem dynamics. Recovery is the reestablishment of a new forest stand or the regeneration of a partially disturbed stand following a previous disturbance. Disturbances occur due to management activities (e.g., harvest), and/or due to abiotic (e.g., windstorm) or biotic (insect pests, diseases) factors. From a management perspective, natural forest disturbances are often considered to cause unforeseen loss of forest biomass or to decrease the actual or potential value of forest stands (Schelhaas, Nabuurs, & Schuck, 2003). However, from an ecological perspective, a natural disturbance is merely a cyclical stage of forest *destruction–creation* dynamics (Moran & Ostrom, 2005; Rull, 2011). The dominant natural disturbance agents in European forests are storm events (53%), fires (16%) and biotic factors (e.g., pest, 16%) (Schelhaas et al., 2003).

* Corresponding author. Tel.: +49 30 2093 6832; fax: +49 30 2093 6848.
E-mail address: magdalena.main@geo.hu-berlin.de (M. Main-Knorn).

0034-4257/$ – see front matter © 2013 Elsevier Inc. All rights reserved.
http://dx.doi.org/10.1016/j.rse.2013.08.010

The Carpathian Mountains sustain Europe's largest continuous forest ecosystem, and are a bridge between Europe's southern and northern forests, serving as an important refuge and corridor for flora and fauna. Carpathian forests provide high biodiversity and productivity, and are a key element of the European carbon cycle (Schulp, Nabuurs, & Verburg, 2008). However, these forests have been influenced by humans for many centuries. During the Austro-Hungarian Empire and expansion of the industrial revolution in the mid-19th century, the demand for energy and fuel increased. As a consequence, exponentially increasing demand for softwood and its products triggered the beginning of regular forest management. Tree species ensuring high productivity, short harvesting cycle and quick revenues were propagated. Thus, most of the natural mountain hardwood and mixed forest stands have been replaced by conifer species, particularly by the productive and "cost-effective" Norway spruce [*Picea abies* (L.) Karst.] (Grodzińska & Szarek-Łukaszewska, 1997; Matiakowska & Szabla, 2007; Turnock, 2002).

In the second half of the 20th century, rapid industrialization, and inadequate environmental regulations led to increased environmental pollution in Central Europe (Csóka, 2005). Long-term critical atmospheric deposition of sulphur and nitrogen caused acidification and eutrophication of ecosystems leading to widespread deterioration of forest health and a diminished resistance to diverse stressors (Kubikova, 1991; Materna, 1989; Schulze, 1989). With the fall of communism in 1989, a phase of institutional and socio-economic changes begun, having direct and indirect impact on Carpathian forests. Direct impact has been observed for instance in Romania, where logging rates triggered by forest privatization and restitution increased (Griffiths et al., 2012; Knorn et al., 2012). Indirect effects linked to forest management and pollution legacies over the last 30 years caused widespread forest decline in the Carpathians (Kubikova, 1991; Main-Knorn, Hostert, Kozak, & Kuemmerle, 2009; Muzika, Guyette, Zielonka, & Liebhold, 2004). Particularly since the late 1990s, forest degradation and mortality of spruce stands reportedly increased in the Western Carpathians (Badea et al., 2004; Grodzki et al., 2004; Kozak, 1996), followed by a decline of forest area at present (Ditmarová, Kmet', Ježík, & Váľka, 2007; Durło, 2010; Grodzki, 2007; Šrámek, Vejpustková, Novotný, & Hellebrandová, 2008). Present forest disturbances in this area result predominantly from the coincidental effects of fungal pathogens (*Armillaria* spp.), unfavorable weather conditions, extreme storm events, and subsequent bark beetle (mainly *Ips typographus* (L.)) outbreaks. Moreover, the observed degradation of spruce stands in the Western Carpathians due to storm events and biotic factors (e.g., insect outbreaks) is expected to increase with climate change in the future (Hlásny, Fabrika, et al., 2010). Thus, assessing the spatial and temporal patterns of disturbances enables determination of past and present degradation and recovery, their long-term trends and potential effect on the carbon balance. It could also improve regional-scale carbon models, provide an important input to model possible impacts of climate change on spruce-dominated forests and underpin new paradigms for management strategies by local and regional policy makers.

As forest biomass dynamics are characterized by disturbances and subsequent recovery processes, the quantification of biomass variability over space and time is critical for accurate carbon accounting (Houghton, 2005). If available, forest inventories based on plot measurements provide biomass estimates with high precision, but these inventory-based approaches are spatially and temporally sparse (Houghton, 2005). Inventories in the Carpathians are designed to provide estimates at the scale of administrative units and for 10-year time intervals. Thus, they are often too coarse in space and time to represent disturbance-induced changes in biomass. Since the net carbon flux of a forest and the magnitude of carbon loss and uptake are determined by the rate of biomass change (reduction or accumulation) at fine spatial and temporal scales, only satellite data can adequately capture its dynamics over larger areas (Huang et al., 2010; Powell et al., 2010; Wulder, White, Coops, & Butson, 2008). Moreover, using time series of remote sensing data both continuous and subtle (associated with forest degradation or recovery) as well as discontinuous and sudden (e.g., clear-cuts, wind-throws) forest change phenomena can be assessed, quantified and monitored (Kennedy, Cohen, & Schroeder, 2007).

The Landsat satellites provide a unique, continuous record of earth observations at ample spatial and spectral resolution since 1972 and, hence, are well-suited for long-term forest change analyses (Cohen & Goward, 2004; Kennedy, Yang, & Cohen, 2010). Moreover, since the recent opening of the Landsat archive by the United States Geological Survey (USGS), new methodological approaches have emerged that make use of annual Landsat time series (Huang et al., 2010; Kennedy et al., 2010). Kennedy et al. (2010) developed a trajectory-based segmentation and fitting method: the Landsat-based detection of Trends in Disturbance and Recovery (LandTrendr), which can be used to reconstruct the disturbance history of forest stands at annual resolution. Unique to LandTrendr is that it detects and describes abrupt disturbances (e.g. fire and harvest) as well as long-term vegetation trends (e.g. regrowth and defoliation). Meigs, Kennedy, and Cohen (2011) applied the LandTrendr algorithm to characterize the impact of insect calamities on tree mortality. In other studies, annual disturbance history trajectories were used to predict forest structure (Pflugmacher, Cohen, & Kennedy, 2012; Pflugmacher, Cohen, Kennedy, & Yang, 2013), and to investigate the effects of institutional and ownership changes on forest resources (Griffiths et al., 2012). Recently, Powell et al. (2010) used LandTrendr to quantify live aboveground forest biomass dynamics at two forested sites in the United States. The authors applied the LandTrendr fitting approach to assess trajectories of biomass change and to reduce inter-annual noise in Landsat-based biomass predictions. The main outcome from this study was that the consistency of Landsat data through time and space made it possible to accurately monitor and quantify trends in biomass.

In a previous study, Main-Knorn et al. (2011) estimated forest biomass in the Western Carpathian Mountains for a single date with satellite and inventory data. Here, we build on the findings of this study and model historic biomass dynamics for the same region at near-annual time steps. To construct near-annual time series, we used imagery from Landsat, Satellite Pour l'Observation de la Terre (SPOT) and Indian Remote Sensing Satellite with the Linear Imaging Self-Scanning Sensor (IRS LISS). Then we use the LandTrendr algorithm to detect and describe biomass trends between 1985 and 2010. The objectives of our study were 1) to map abrupt and gradual disturbances, and forest recovery in the spruce-dominated forests of the Western Carpathian Mountains, 2) to quantify biomass losses and gains associated with these processes, and 3) to quantify the net change in forest biomass within the observation period.

2. Study area

The study area covers ~116,000 ha of forested land in the Beskid Mountains of the northwestern Carpathian Mountain Range (Fig. 1). Here, we focused on coniferous forests which encompass ~56,000 ha of the total forested area. Elevations in the study region extend up to 1550 m above sea level in the Beskid Żywiecki Massif. The climate is typical for moderate continental mountain zones with an annual precipitation of 1200 mm (Durło, 2010). The yearly mean temperature is about 7 °C below 700 m and about 4 °C at 1100 m. The dominant wind directions are western, south- and northwestern, with the highest speed between November and March potentially causing great damage to forest stands (Barszcz & Małek, 2008). Warm foehn winds from the south and southwest as well as temperature inversion in valleys are important aspects of the regional climate.

The dominating forest types are Norway spruce monocultures and mixed spruce stands with the admixture of European beech (*Fagus sylvatica*) and European silver fir (*Abies alba*) (Barszcz & Małek, 2008). As a result of ongoing stand conversion, some lower elevations feature mixed beech forests along with spruce and fir.

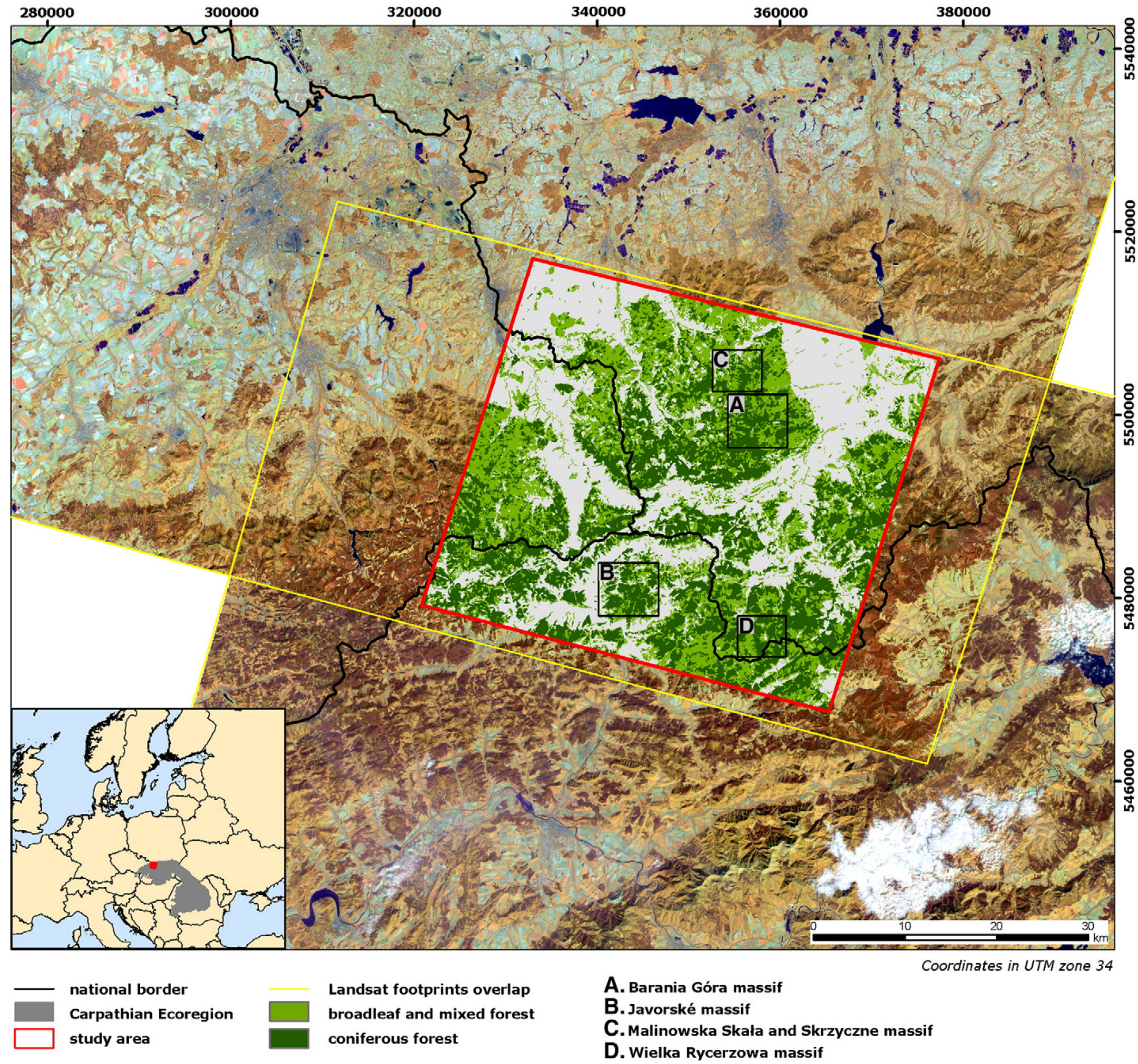

Fig. 1. Study area within the Beskid Mountains in the border region of Poland, the Czech Republic and Slovakia, with four sub-areas: Barania Góra massif in Poland (A), Javorské massif in Slovakia (B), Malinowska Skała and Skrzyczne massif in Poland (C), and Wielka Rycerzowa massif along the Polish–Slovak border (D).

3. Data and methods

Our study region is covered by two Landsat footprints (path/row: 189/25 and 188/26). We acquired a near-annual time series of Landsat Thematic Mapper (TM) and Enhanced Thematic Mapper Plus (ETM+) images for the period 1985–2010 (Fig. 2). For 2009 only ETM+ images with data gaps caused by a failure of the sensor's scan-line-corrector (SLC) were available. To fill these data gaps, we used three adjacent images acquired in the same year (path/row: 189/25, 188/25, 188/26). Further, due to the limited availability of Landsat data for the study region between 1996 and 1999 (caused by data transfer regulations and affected many regions of the world (Goward et al., 2006)), we also included imagery from SPOT-1 (path/row 73/249) and IRS LISS-III (path/row 33/33) for the years 1997 and 1998, respectively. These sensors have spatial and spectral properties similar to Landsat, and have been used in other Landsat-based time-series studies (Hill & Aifadopoulou, 1990; Huang et al., 2010; Powell, Pflugmacher, Kirschbaum, Kim, & Cohen, 2007; Wilson & Sader, 2002). The SPOT-1 image consists of three spectral bands from the green (0.50–0.59 μm), red (0.61–0.68 μm), and near-infrared (0.78–0.89 μm) wavelengths of the electromagnetic spectrum, with a pixel resolution of 20 m. The IRS-C1 LISS image features two visible bands (0.52–0.59 μm and 0.62–0.68 μm) and one near-infrared band (0.77–0.86 μm) with a 23.5 m spatial resolution, and one short-wave infrared band (1.55–1.70 μm) with a 70.5 m pixel resolution.

3.1. Satellite data preparation

Geometric and radiometric normalization of time series images are crucial for any type of change detection over time (Lu, Mausel, Brondizio, & Moran, 2004). We used geometric and radiometric processing techniques described in detail by Schroeder, Cohen, Song,

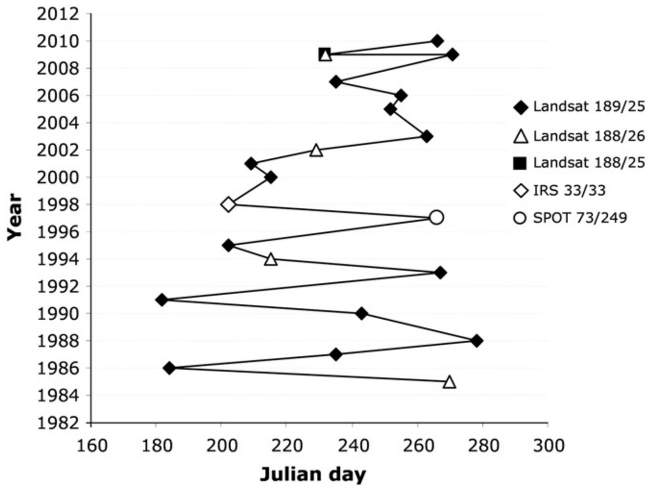

Fig. 2. Scene acquisition dates by year, path and row and the sensor type. Julian days were calculated relative to January 1st.

Canty, and Yang (2006). Briefly, geometric correction was based on an automated generation of image tie points (Kennedy & Cohen, 2003) between the reference (here the orthorectified 2001 L1T image) and the respective input image. After more than 300 tie points were identified, a polynomial transformation was used to spatially align the images. SPOT and IRS LISS images were resampled using cubic convolution interpolation to the 30 m spatial resolution matching the Landsat images. Co-registration between images resulted in an overall positional error of <0.5 pixels.

The cloud-free 2003 image was atmospherically corrected using the COST method (Chavez, 1996). All other images (Landsat, SPOT and IRS LISS) were radiometrically normalized to the corrected 2003 image using the MADCAL (Multivariate Alteration Detection and Calibration) algorithm from Canty, Nielsen, and Schmidt (2004). The MADCAL algorithm identifies no-change pixels between image pairs and normalizes each image to a reference image using orthogonal regression (Schroeder et al., 2006). Since our study focused on coniferous forest, we created a conifer forest mask for the years 1987 and 2005 (the last year before mass insect outbreaks and related widespread forest decline) using Support Vector Machine (SVM) classification (Pal & Mather, 2005) and a procedure outlined in Main-Knorn et al. (2009). Finally, clouds and cloud shadows were digitized and masked. Clouds and shadows were identified on 11 images of the time series, of which seven clouded scenes occurred between 2000 and 2009. The average cloud and cloud shadow coverage was about 7% of the study area, and ranged from 1% of the study area in 1990 to 17% in 1991.

SPOT-1 data consist of three spectral bands (two visible bands and one near-infrared band), with similar characteristics to Landsat TM. However, unlike Landsat and IRS LISS, SPOT-1 does not include a short-wave infrared (SWIR) band, which is particularly useful for detecting forest changes. Moreover, in a previous study, SWIR was one of the most important explanatory variables for predicting biomass (Main-Knorn et al., 2011). Hence, we considered alternative options to cope with the lack of SWIR by modeling a pseudo-SWIR band for SPOT. Using 1000 training samples from Landsat 1995 image, we built a linear regression model to predict Landsat TM SWIR (band 5) from two visible bands and one near-infrared band (Landsat bands: 2, 3, and 4, respectively). We tested and validated the model on the 1995 image and on the cloud-free image from 1992. The model (strong and statistically significant with $P < 0.001$ and R^2 of 0.9) was then applied to the corresponding three SPOT-1 bands to predict the pseudo-SWIR band. The created SWIR band and remaining SPOT bands were stacked and included in the Landsat time-series.

3.2. Biomass estimation and model validation

Satellite image time series, field inventory data and the biomass modeling technique based on Random Forests (RF) were used to create near annual biomass maps over 25 years. A detailed description of RF can be found in Breiman (2001), Prasad, Iverson, and Liaw (2006) and Cutler et al. (2007). The RF application for remote-sensing based biomass modeling was introduced by Main-Knorn et al. (2011). Therefore, in the following we provide only a brief description of the modeling and modification details.

3.2.1. Field data

We calculated total live aboveground forest biomass (AGB) from forest inventory (FI) data provided by 'The State Forests National Forest Holding'. Inventories were conducted in 2003, 2004 and 2007. First, 211 randomly selected FI plots were verified during field surveys in 2005, 2006 and 2007 (Main-Knorn et al., 2011). Then, we converted the growing stock volume to AGB [Mg ha^{-1}] for these FI plots using equations for Carpathian Norway spruce forests (Lakida, Nilsson, and Shvidenko (1996)) as follows:

$$\mathrm{AGB} = \mathrm{V_{st}} * \mathrm{R_{v(ab)}} \tag{1}$$

where V_{st} in the growing stock of stemwood [m^3 ha^{-1}], and $R_{v(ab)}$ is the ratio between aboveground standing biomass and the volume of the growing stock over bark. The ratio was calculated as:

$$\mathrm{R_{v(ab)}} = a_0 * A^{a_1} \tag{2}$$

where A is stand age [years], and a_0 and a_1 are spruce-specific regression coefficients equaling 2.058 and −0.383, respectively (Lakida et al., 1996). The observed forest biomass ranged between 0 and 300 Mg ha^{-1}, including unstocked plots located in forest meadows and clear-cuts.

3.2.2. Biomass models

Using the 3 × 3 pixel mean of spectral data from the 2005 image (closest to the FI data acquisition), terrain information (DEM from the Space Shuttle Radar Topography Mission (SRTM) resampled to 30 m spatial resolution), and the plot-level AGB data, we derived two separate RF biomass models based on: (A) six Landsat bands, terrain slope, and direct solar radiation (dsr) (Davis & Goetz, 1990; Fitterer, Nelson, Coops, & Wulder, 2012), and (B) the same variables but excluding bands 1 (VIS blue) and 7 (SWIR II) (Table 1).

Table 1
Model description and cross-validated results for biomass modeling. RF parameter Ntree corresponds to the number of regression trees to grow, and Mtry is the number of explanatory variables selected at each node.

	Variables								Model parameter		Accuracy assessment	
	VIS blue	VIS green	VIS red	NIR	SWIR I	SWIR II	dsr	Slope	Ntree	Mtry	r	RMSE
Model A	x	x	x	x	x	x	x	x	1500	5	0.8	40.1
Model B		x	x	x	x		x	x	1000	3	0.79	41.3

The evaluation of the models was based on a 10-fold cross-validation. We also calculated for every model: Pearson's correlation between observed and predicted values, and the root mean squared error (RMSE). We applied model (A) to the Landsat images and model (B) to the SPOT and IRS images to create AGB maps for each image in the time series. Because all images had been radiometrically normalized, it was possible to apply the derived RF models to all images in the time series (Powell et al., 2010). However, we checked the robustness of the models across different Landsat footprints and different sensors (Landsat, SPOT-1, IRS-LISS). For this purpose, we used 50 no-change samples (stable forest) from a previous study (Main-Knorn et al., 2009), where time period 1987–2005 was considered. These samples were identified using forest inventory and available aerial photography or satellite data. The same pixels were selected from the Landsat-, SPOT- and IRS LISS-based AGB maps between 1993 and 2005. Using the mean value of the 3 × 3 pixel window surrounding each no-change pixel per year, the standard deviation of the biomass predictions was calculated and its distribution plotted.

3.3. Trajectory analysis

To map disturbance and recovery trends we applied the LandTrendr temporal segmentation and fitting algorithm to the biomass predictions. Thus, all biomass maps were first assembled into a stack of biomass time series. The temporal segmentation algorithm then delineated a single segment (gradual decrease, increase, stable) or sequences of segments (here we used up to six to characterize multiple processes) for each pixel, capturing biomass change over time, while minimizing year-to-year noise caused by illumination or phenology. The fitting procedure derives simplified trajectory sequences of segments, using regression-based and point-to-point fitting algorithms (Kennedy et al., 2010). Gaps in the biomass time series related to clouds, cloud shadows and general data scarcity were linearly interpolated.

To summarize the variety of disturbance and recovery trajectories occurring across all pixels in the study region, LandTrendr provides four parameters: onset year of change events, relative (biomass) magnitude of change (%), duration (number of years), and biomass value prior to the change event. Because LandTrendr uses thresholds of percent vegetation cover to minimize detection of false changes, we converted the absolute biomass values from Mg ha^{-1} (AGB_i) to percent biomass ($rAGB_i$) to provide such a forest cover approximation. $rAGB_i$ was calculated as:

$$\mathtt{rAGB}_{\mathtt{i}} = \left(\frac{\mathtt{AGB}_{\mathtt{i}} - \mathtt{AGB}_{\mathtt{min}}}{\mathtt{AGB}_{\mathtt{max}} - \mathtt{AGB}_{\mathtt{min}}}\right) * 100 \tag{3}$$

where '$AGB_{max} - AGB_{min}$' was the range of biomass estimates for the entire coniferous area.

$rAGB_i$ was then used to calculate the relative magnitude (M_{rel}) of biomass change as follows:

$$\mathtt{M}_{\mathtt{rel}} = \frac{100 * \left(\mathtt{rAGB}_{\mathtt{pre}} - \mathtt{rAGB}_{\mathtt{post}}\right)}{\mathtt{rAGB}_{\mathtt{pre}}} \tag{4}$$

where $rAGB_{pre}$ and $rAGB_{post}$ are relative biomass before and after disturbance, respectively. Then, we used percent of biomass range to define a minimum detection threshold (20% for abrupt disturbances, 5% over 20 years for gradual decreases).

3.4. Mapping forest biomass loss, accumulation, total and net biomass change

We were interested in four main change processes: abrupt biomass loss, gradual biomass decrease, gradual biomass increase, and stability (no change). Each of these processes can be represented by a single segment in the biomass trajectory. However, often more than one process occurred within the 25-year period (Fig. 3). We defined the following classes to describe dynamic processes through trajectories:

- disturbance: an abrupt event that causes the loss of live forest biomass over a period of up to three years (Fig. 3A (year 2000) and Fig. 3B (2006)),
- gradual decrease: biomass loss over more than three years (Fig. 3A, until 1999),
- disturbance followed by recovery (Fig. 3A (after 2000) and Fig. 3B (after 2006)),
- gradual decrease then recovery,
- gradual increase (biomass accumulation in undisturbed forests — Fig. 3C).

The differentiation between abrupt and gradual disturbances enabled us to assess different processes: abrupt events in the study region may represent clear-cuts and wind-throws, and gradual biomass loss may represent forest degradation (e.g., defoliation, yellowing) caused by diseases or insects. Selective logging is an abrupt change but in cases of repeated, low-intensity logging it may be mapped as longer-duration biomass loss.

We created four maps to analyze the spatial patterns of biomass change throughout the study area: a disturbance onset map, a total gradual decrease and increase map, a recovery onset map, and a net biomass change map. To summarize disturbance rates and patterns, we calculated the total disturbed area per year and for 5-year periods, splitting disturbance rates equally for missing data among adjacent years. Similarly, we summarized the total disturbed area per year for gradual biomass changes. "Year" here refers to the first year of gradual biomass decrease or increase as gradual change is a continuous process.

We classified biomass loss on the pixel level to be "severe", "moderate" and "low" when M_{rel} of biomass change was above 75%, 50–75%, and below 50%, respectively. Finally, net biomass change for each pixel was estimated by subtracting the biomass value predicted for 1985 from the biomass value predicted for 2010. Thus, a positive net change corresponded to a net increase in biomass and a negative net change corresponded to a net decrease in biomass over the 25 year period. Pixels with a net change between −20 and 20 Mg ha^{-1} were considered no change and replaced with zeros.

3.5. Establishing recovery and a gradual biomass increase trajectories

We calculated net biomass increase per pixel associated with forest recovery after abrupt and gradual disturbances, based on the magnitude of the recovery. Then, we selected only pixels that underwent a stand-replacing disturbance (post-disturbance biomass levels below 10 Mg ha^{-1}) and calculated the annual mean recovery rate and mean recovery trajectories over a 15-year period. Similarly, we summarized the annual biomass accumulation rates and coniferous gradual increase trajectories over 25 years. In addition, using meteorological data provided by the Czech and Polish Hydrometeorological Institutes, we examined the relationship between biomass accumulation rates, mean air temperature and monthly precipitation to explore spruce growth responses to climate variables.

3.6. Assessment of the LandTrendr results

To examine the veracity of the LandTrendr results, we used the visualization and data collection tool TimeSync (Cohen, Yang, & Kennedy, 2010). TimeSync simultaneously visualizes time series of image chips from the analyzed satellite data and from high-resolution imagery available in Google Earth. A trajectory window displays the corresponding averaged reflectance per 3 × 3 pixel plot for all image chips, allowing for a synoptic interpretation of spectral changes over time.

We selected a reference dataset based on a stratified random sample to evaluate the disturbance map. We collected 290 reference points for the "abrupt disturbances" class, and allocated them proportionally in a

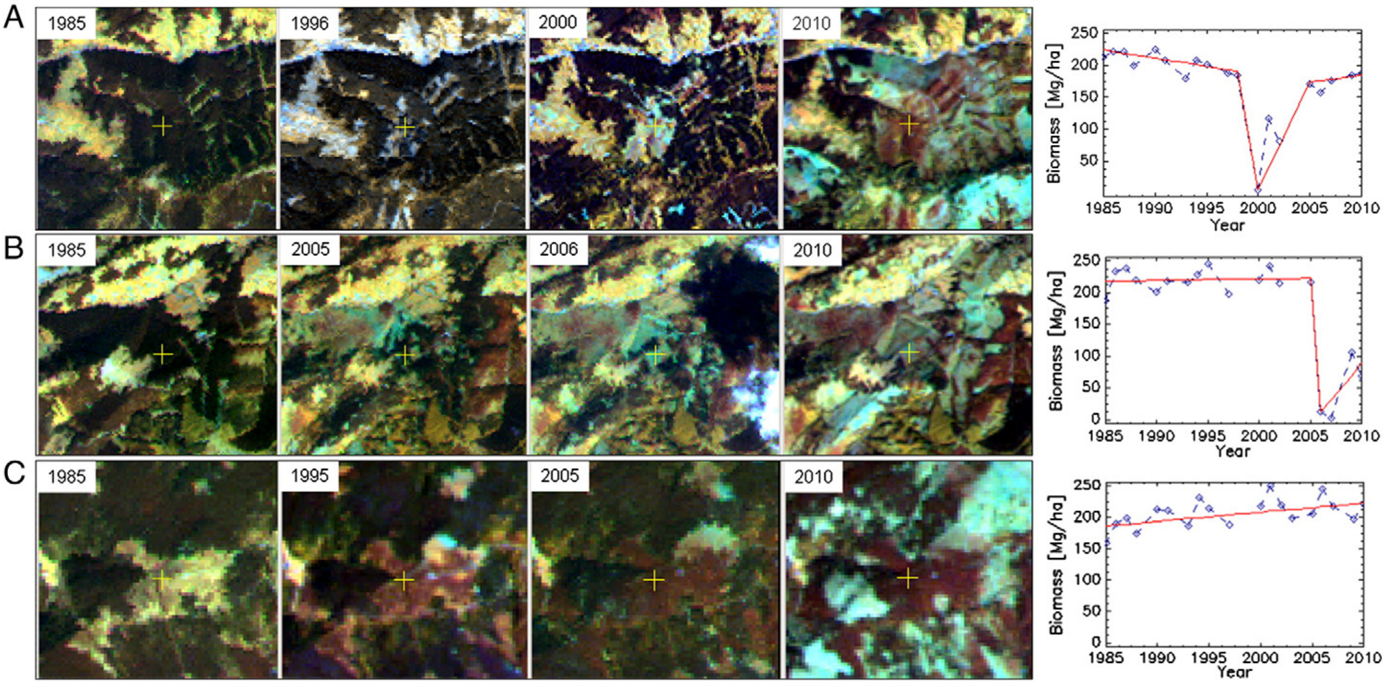

Fig. 3. Three examples of source values (blue), fitted trajectories (red), and related imagery (R–G–B = TM bands 4–5–3). Fitted trajectories represent change classes: gradual decrease–disturbance–recovery (A); no change–disturbance–recovery (B); gradual increase (C). Trajectory locations are indicated by the yellow crosshair. Gaps in source value trajectories indicate masked no-data values.

class-wise stratified manner (19 years = 19 classes), after eliminating patches of two pixels or less. We assigned a maximum number of 20 samples to the largest class (year 2009) and a minimum of 5 samples to those classes that had an area below 1%. The number of samples for classes in-between was linearly scaled. In addition, a sum of 397 points was randomly sampled and proportionally allocated for long-term gradual biomass changes (decrease, recovery, and increase) and the no-change class. In total, 687 samples were selected for evaluation purpose. Using TimeSync, we recorded the onset year of abrupt disturbances. Gradual biomass changes were interpreted by simultaneously assessing satellite images and temporal reflectance trajectories. When the normalized time-series reflectance values of band 5 showed a continuously decreasing trend over a period of more than three years, the pixel was interpreted as gradual biomass decrease. In contrast, continuously increasing reflectance values over 25 years were associated with the "gradual biomass increase" class. When a marked decrease in the reflectance was followed by a reestablishment in reflectance, a pixel was validated as "biomass recovery". We compared the LandTrendr change results against the TimeSync reference database and calculated an error matrix. We derived overall accuracy and omission and commission errors, accounting for sampling bias and providing true class area estimates as well as the 95% confidence intervals around those estimates (Card, 1982; Cochran, 1977) .

4. Results

4.1. Biomass models

The estimation of forest aboveground biomass was robust, having a RMSE of 40 Mg ha^{-1}, and a correlation coefficient of 0.8 based on the Model A. Estimates based on Model B were almost equally accurate, showing an r of 0.79, and a RMSE of 41.3 Mg ha^{-1} (Table 1). The no-

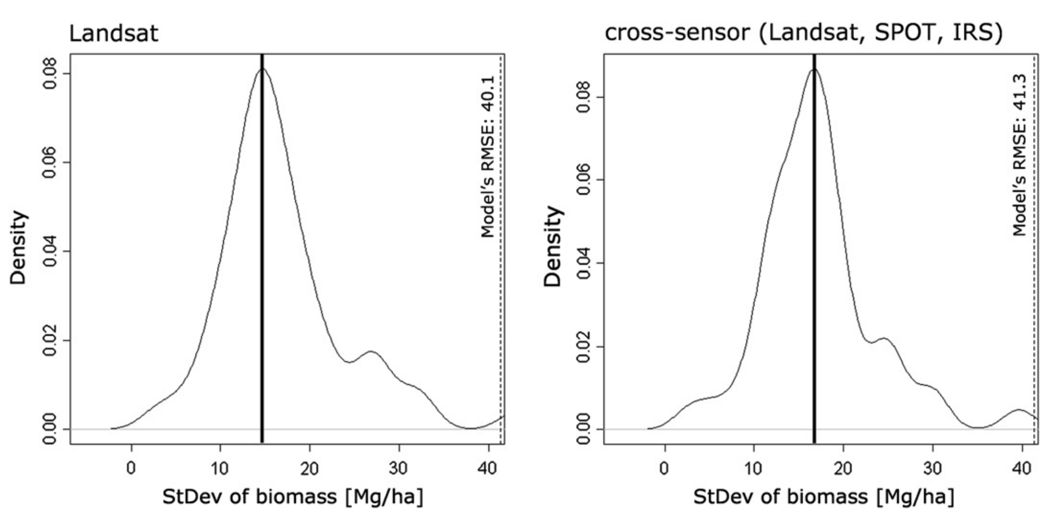

Fig. 4. Density plots — distribution of the standard deviation for no-change biomass pixels; Left: Stdev distribution between 1993 and 2005 for model A (Landsat only; 1997 and 1998 excluded); Right: Stdev between 1993 and 2005 for both models A and B (based on Landsat; SPOT and IRS LISS).

change pixels extracted between 1993 and 2005 showed a generally low standard deviation of annual biomass estimates (Fig. 4). Density peak reached 14 Mg ha^{-1} for Landsat time series, and 17 Mg ha^{-1} for cross-sensor time series (including Landsat, SPOT and IRS LISS data), which is clearly below the RMSE of the RF model.

4.2. Map accuracy

LandTrendr produced accurate disturbance maps with an overall accuracy of 83.33% (Table 2). The stable forest (no change class - NC) and gradual decrease class (GD) showed omission and commission errors below 20%, respectively. The recovery class (REC) achieved almost 20% higher producer's and user's accuracies than the gradual increase class (GI). Commission errors for the annual disturbance classes were generally low (mean = 16.9%, standard deviation = 15.6%) with lower errors in the years 1987, 1988, 1990 and 2001, and higher errors in the years 2002 and 2003. In comparison, omission errors were higher (mean = 20.6%, standard deviation = 24.8%) in 1987 and 2005 (Table 2).

4.3. Biomass loss vs. abrupt and gradual disturbances

Overall, ~45% (~25,000 ha) of the total coniferous forests showed stability or steady increases in biomass over the past 25 years. Thus, a substantial area (55% of the total coniferous area) experienced a loss of biomass at some time during the observation period caused by gradual or abrupt disturbances. Gradual disturbances dominated (~50% of all disturbances), affecting ~13,600 ha of coniferous area. Abrupt changes constituted about 37% of all disturbances, and remaining 13% reflected area, where abrupt disturbance was preceded by gradual disturbance.

Abrupt disturbances caused loss of biomass across the entire study area, with several hot spots along a north–south gradient and crestline (Fig. 5). Further, these disturbances increased exponentially during the observation period (Fig. 6A). The vast majority of the disturbed area (82%) was disturbed between 2005 and 2010. For the same time period, 55% of the affected area underwent severe disturbances; a substantially higher proportion compared to previous time periods (Fig. 6B). Moderate abrupt disturbances were observed for about 20% of the total disturbed area between 1985 and 1999, and decreased slightly from 20% to 15% between 2005 and 2010, while low and moderate disturbances dominated the period between 2000 and 2004.

As reported before, biomass loss caused by gradual disturbances affected 13% more coniferous area compared to abrupt disturbances. Long-term biomass decrease was more evenly distributed across the entire study area. However, areas with moderate and severe biomass decrease were observed in the same part of the study area as abrupt biomass loss (Fig. 7-I). In most cases, the onset year of gradual decrease appeared in the very beginning of our time series; however, we also observed a second culmination between 2000 and 2004 (Fig. 6C). The fractions of severe and moderate biomass loss increased from 8% to 35% over time, whereas the proportion of low to moderate change intensity declined (Fig. 6D). Overall, low to moderate intensity of biomass decrease dominated across all years. Regarding the duration of gradual biomass decrease, most changes occurred over no more than ten years, while a considerable area (~5200 ha) exhibited a biomass decrease over the entire study period (Fig. 6F).

Table 2
Accuracy assessment for the biomass change classes: stable forest (no change — NC), biomass disturbance onset year, and the gradual biomass change classes gradual decrease (GD), recovery (REC), and gradual increase (GI). Error of omission (O), error of commission (C), and overall accuracy (OAC).

Class	O	C
1986	0.00%	36.36%
1987	96.72%	0.00%
1988	0.00%	0.00%
1990	20.03%	0.00%
1991	11.94%	9.09%
1993	0.00%	16.67%
1994	42.57%	25.00%
1995	31.76%	16.67%
1997	0.00%	25.00%
1998	3.12%	20.00%
2000	19.28%	15.38%
2001	39.15%	0.00%
2002	13.38%	53.33%
2003	18.72%	50.00%
2005	56.90%	8.33%
2006	0.00%	9.52%
2007	23.83%	9.52%
2009	14.87%	13.04%
2010	0.00%	12.50%
GD	19.21%	7.89%
REC	13.57%	24.32%
GI	30.82%	45.71%
NC	14.70%	15.26%
OAC	83.33%	

4.4. Biomass accumulation

Only about 20.5% of the total disturbed area showed a recovery in biomass (11.2% of conifer forest compared to 55% disturbed). This recovery was mainly observed in areas that previously experienced abrupt disturbance (8.7% of coniferous, and 77.8% of total recovery area). Hence, only small proportion of area affected by gradual disturbances actually recovered (2.5% of coniferous area compared to about 24% gradually disturbed). For more than 70% of all recovery pixels, the recovery started between 2000 and 2010 (Fig. 6E, Fig. 7-II).

Regarding recovery trajectories, there were no considerable differences in recovery characteristics between gradual and abrupt disturbances. The average recovery trajectory and the annual recovery rates signaled intensive biomass increase, particularly within the first five recovery years (annual recovery rates up to 17 Mg ha^{-1} yr^{-1} decreasing after the first five years below 10 Mg ha^{-1} yr^{-1}). Biomass recovered from about 10 Mg ha^{-1} for the post-disturbance stage (stand-replacing disturbances) to 155 Mg ha^{-1} of aboveground biomass after the 15th recovery year. The mean gradual increase trajectory for the 25-year period indicated a biomass increase from 156 Mg ha^{-1} in 1985 to 217 Mg ha^{-1} in 2010. The annual accumulation rates were constant and reached 2.5 Mg ha^{-1} yr^{-1} (+/−0.04 Mg ha^{-1}) of biomass increase.

4.5. Total and net biomass change

The total coniferous biomass decreased by 15% (17 Mio Mg) between 1985 and 2010.

The net biomass change map (Fig. 8) shows a net decrease in biomass on 38% of the coniferous area, whereas a positive net change accounted for only 8.4%. Biomass decreased most strongly (>100 Mg/ha) for 15.7% (~8818 ha) of the coniferous stands, whereas only 0.6% of the coniferous area showed a net increase in AGB greater than 100 Mg/ha. The maximum negative net change reached −302 Mg ha^{-1}, and the highest positive net change equaled 304 Mg ha^{-1}. The mean net biomass change for the study area was −36.2 Mg ha^{-1}. The frequency of negative biomass change showed two modes at −38 Mg ha^{-1} (694 ha of total coniferous area) and −215 Mg ha^{-1} (~293 ha), respectively.

5. Discussion

Modeling biomass trajectories using the LandTrendr algorithm revealed a dramatic decline in aboveground forest biomass between 1985 and 2010, affecting almost 55% of the total coniferous forest in the Western Carpathians study region. The area affected by stand-replacing disturbances and long-term degradation increased exponentially, and this process peaked during the last five years of the analysis

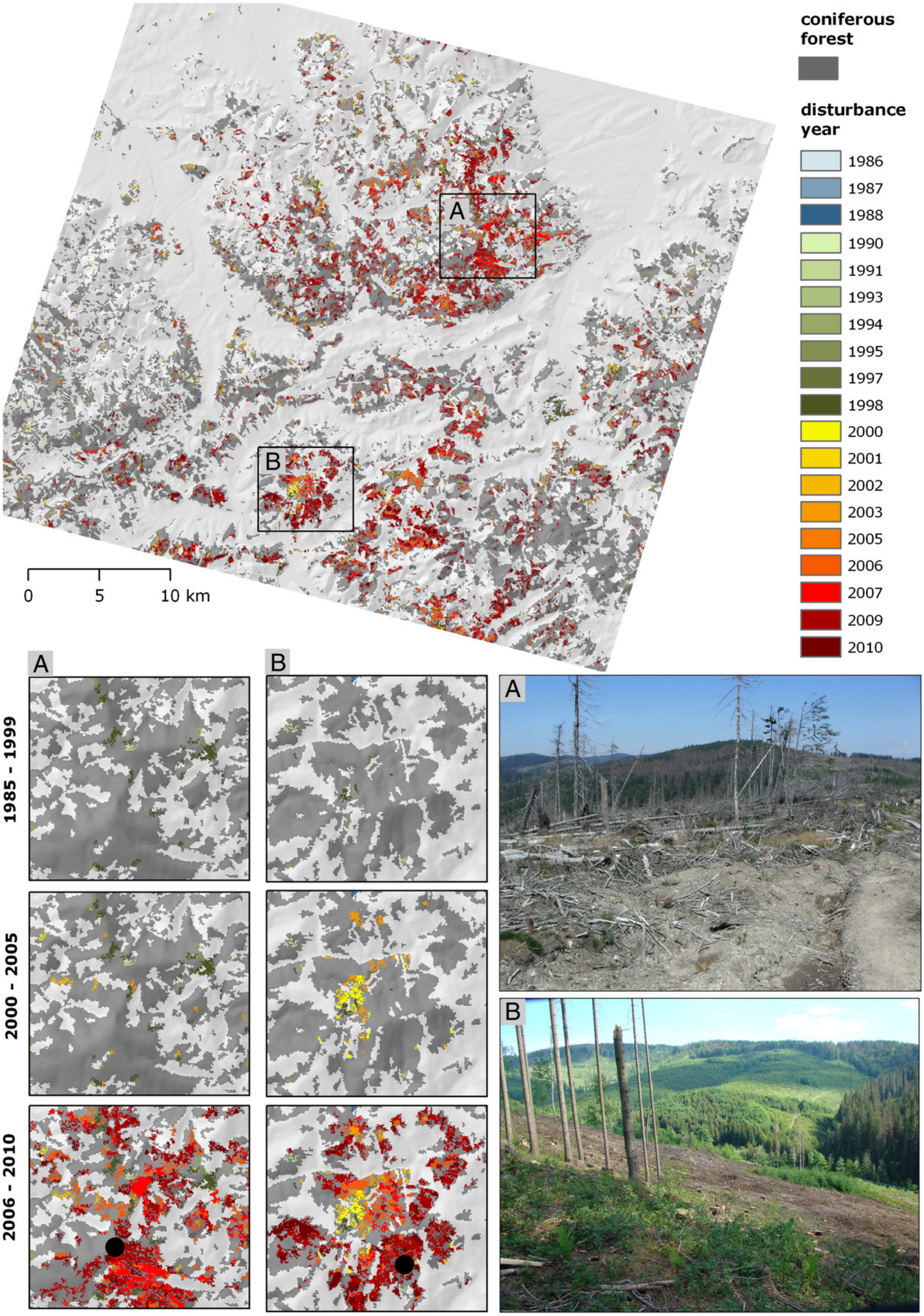

Fig. 5. Disturbance map with highlighted sub-areas (A) and (B), and corresponding photographs taken in 2007 (source: J. Kozak) and 2009 (source: L. Kulla), respectively (black dots).

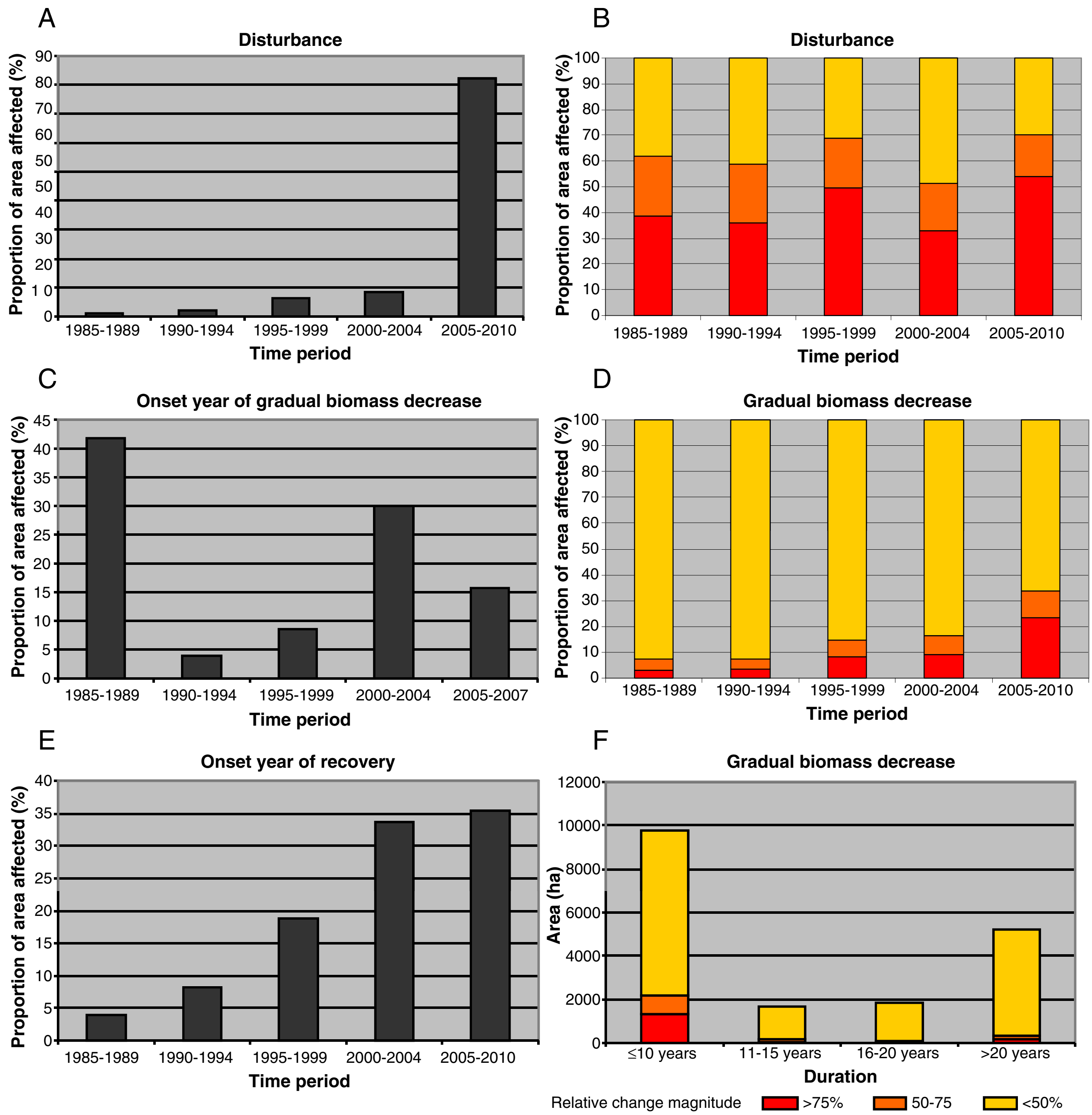

Fig. 6. Time dependency of disturbances (A) and corresponding relative magnitude of severe, moderate and low biomass loss (B); onset year of gradual biomass decrease (C) and corresponding distribution of the relative magnitude classes (D); recovery onset year distribution (E); proportion of the relative magnitude classes along with duration of gradual biomass decrease (F).

period. This corroborates reported increases in salvage cuttings for the Slovak, Polish and Czech part of the Western Carpathians, particularly since 2005 (Hlásny, Grodzki, Šrámek, et al., 2010), and decreasing coniferous forest cover (Main-Knorn et al., 2009). Substantial biomass loss since 2005 caused by insects and fungal pathogens, and considerable surplus of salvage cuttings (Grodzki, 2012) amplified the negative balance of net forest biomass change. Consequently, the results suggest that the losses of coniferous biomass were not balanced by the gains in our study area during the observation period.

The observed severe and widespread loss of biomass in the study area was likely caused by a few consecutive or simultaneously occurring biotic and abiotic drivers. Low resistance of spruce occurred due to unfavorable forest composition and foreign species ecotype. The propagation of Norway spruce in mid-19th and the 20th century caused large replacement of natural fir and beech forests by spruce monocultures of foreign origin, particularly in the Western Carpathians (Capecki, 1994). Weakened spruce was then affected by long-term critical atmospheric deposition of sulphur and nitrogen leading to direct damage of trees, as well as degradation of soil chemistry and extinction of soil microorganisms. In consequence, the natural symbiotic forest ecosystem was damaged and could no longer provide protective functions for the trees (Hlásny & Sitková, 2010; Matiakowska & Szabla, 2007). Effects on trees could be observed either immediately (through discoloration and defoliation), or delayed causing long-term loss of vigor and elevated activity of fungal pathogens (*Armillaria* spp.) (Longauerová, Leontovyč, Krajmerová, Vakula, & Grodzki, 2010). Our results show both, an abrupt and a long-term gradual biomass loss since 1985, while the latter corresponds to 50% of the total disturbed

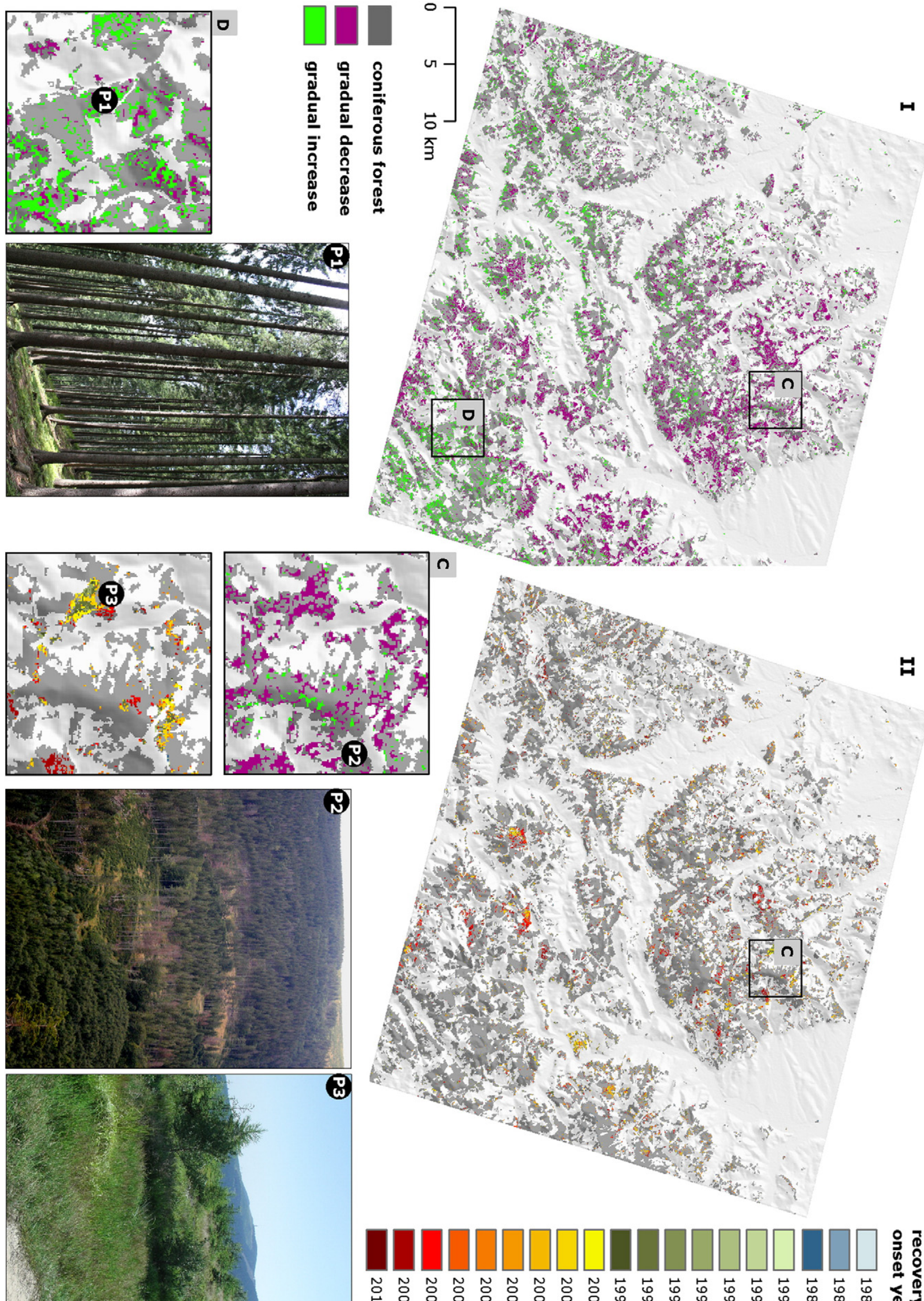
I
II
C
D
P1
P2
P3
0 5 10 km
coniferous forest
gradual decrease
gradual increase
recovery onset year
1986
1987
1988
1990
1991
1993
1994
1995
1997
1998
2000
2001
2002
2003
2005
2006
2007
2009
2010

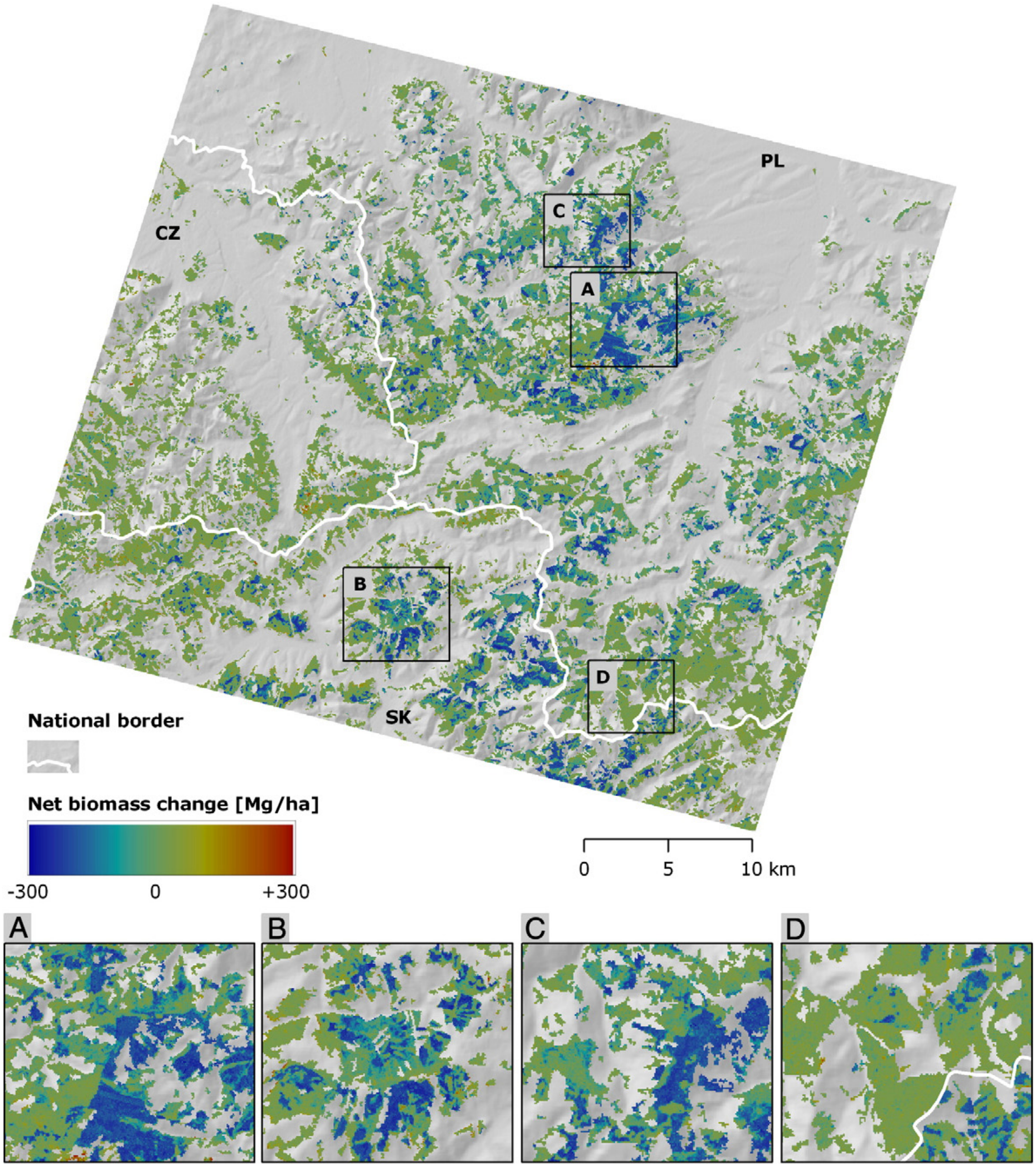

Fig. 8. Net biomass change map with sub-areas: Barania Góra massif (A), Javorské massif (B), Skrzyczne massif (C), and Wielka Rycerzowa massif (D).

area. Moreover, subsequent gradual and abrupt disturbances affected 13% of the total disturbed forest.

We show that moderate to severe biomass loss, both abrupt and gradual, has been constantly increasing (Fig. 6A, B and D), which could be explained by: 1) markedly delayed response of the soil environment to long-term atmospheric toxic loads, and 2) a decreasing resistance of spruce stands against biotic and abiotic factors since the early 1990s (Mijal & Kulis, 2004). On the one hand, less resistant spruce was susceptible for fungal diseases and bark beetle infestation; on the other hand, adverse climate conditions with subsequent extreme weather events occurred. Particularly, this coincidental effect can be shown in two sub-regions: the Barania Góra massif in Poland (A) and the Javorské massif in Slovakia (B) (Fig. 5). The first example delineates two time peaks of biomass loss, first in the late 90s and second, about ten years later (Fig. 5A). Both peaks were biotically-induced (fungal pathogens and bark beetle), while the second event (still ongoing) has been additionally accelerated by unfavorable weather conditions (physiological and summer drought) and a windstorm in 2004. Between 1995 and 2005 abrupt biomass change occurred on relatively small patches that were widespread along an elevation gradient. In contrast, disturbances between 2006 and 2010 affected a continuous forest area and caused a tremendous biomass loss along the entire elevation gradient. A second example, the area of the Javorské massif (B), reflects ongoing forest disturbances which begun in 2000. Here, the initiating driver in 2000 was the activity of a pathogenic fungus (*Armillaria* spp.) followed by bark beetle infestation since 2005 (Hlásny &

Fig. 7. Gradual biomass change maps. Gradual decrease and increase (I) and recovery onset year (II). Two example areas (C and D) and corresponding photographs (P1 and P2 — source: M. Main-Knorn 2006; and P3 — source: J. Kozak 2006) demonstrate gradual increase in biomass (D and P1), long-term gradual biomass loss (I-C and P2), and recovery processes (II-C and P3).

Sitková, 2010). Similar to biomass loss on the Barania Góra massif, extreme weather conditions in 2003 and 2004 accelerated extensive bark beetle outbreaks (Grodzki, 2010). In this case, the biomass loss is likely to be a continuously and gradually developing process, starting as distinct patches on the mountain peaks and then spreading downhill.

Although both examples differ in terms of temporal and spatial disturbance onset, recent biomass loss seems to have the same reasons and progress. Intensive salvage logging was conducted after the windstorm and fungal activity in November 2004, leaving a large amount of dead wood suitable for bark beetle breeding and reproduction. Simultaneously, a mild winter and dry growing season in 2003 and following years facilitated increased insect survival and reproduction, boosting outbreaks in the surrounding stands (neighborhood effect, compare Fig. 5). Finally, once the bark beetle population has reached a critical size, it affects whole stands and damages trees independently of their health status (Hlásny, Grodzki, Turčáni, Sitková, & Konôpka, 2010).

Generally, only about 20.5% of the total disturbed area showed a recovery in biomass. This can be partially related to the intensive disturbances since 2005, leaving not enough time for regeneration. The recovery map (Fig. 7-II) gives an overview on this scarce regeneration, and the example area C demonstrates recovery processes after long-term gradual biomass loss until the mid-90s followed by abrupt biomass loss (disturbances) (Fig. 7-II C). Slow reestablishment of new forest cover is organized in compact patches, suggesting intensive silvicultural measures. For this pattern, there are two explanations. First, although natural regeneration of spruce has proven feasible in several locations of the study area, its quality, vitality and survival chances are not sufficient to guarantee continuous spruce forest expansion above 800 m (Barszcz & Małek, 2008). Moreover, adverse site- and weather conditions limit the intensity of spruce seed production and thus natural regeneration (Longauer, Gömöry, Pacalaj, & Krajmerová, 2010). Therefore, recovery has to rely on artificial regeneration of spruce using seeds of local origin (provenance) (Barszcz & Małek, 2008; Slodičák, Novák, Štefančík, & Kamenský, 2010). Second, critical biomass loss in the study area forces forest managers to develop a stable and close-to-nature forest, consisting of European beech, silver fir, sycamore maple (*Acer pseudoplatanus* L.), and admixture of Norway spruce (Slodičák et al., 2010). These species are promoted and artificially introduced on previously damaged stands, but also as conversion of existing spruce monocultures. However, as silvicultural measures are time- and work consuming, and are hampered by adverse site and weather conditions in our study area, low recovery rates seem to be comprehensible.

Our averaged recovery trajectory shows biomass increase after stand-replacing disturbance to 155 Mg ha^{-1} of aboveground biomass after 15 recovery years. However, note that recovery here primary relates to general vegetation reestablishment (not necessarily conifer growth) as an early succession stage. The recovery curve and the rates indicate intensive biomass increase, particularly within the first five recovery years, and slight slowdown of growth for the subsequent years. These findings are in line with the general knowledge of forest reestablishment in a temperate zone, arising shortly after disturbance and expanding quickly before leveling off (McMahon, Parker, & Miller, 2010). Although we were not able to observe the mentioned leveling off due to our short observation time, we were able to assess the variability of recovery rates in the early succession stage, indicating a high complexity of the recovery process due to external factors. Better understanding of temporal patterns of forest regeneration and their drivers requires detailed knowledge of the site- and micro-climate conditions, as well as silvicultural measures at the stand level. Because spatial patterns of recovery are in line with the disturbance history and known silvicultural approaches, and because the averaged recovery trend confirms our expectation, we propose that the trajectory-based analysis provides comprehensive spatio-temporal information on the reestablishment of new forest.

The small proportion of coniferous area characterized by steady increase in biomass makes these forests particularly interesting for investigation. As exemplified in the Wielka Rycerzowa massif (D), coniferous biomass has gradually increased and these stands remain in a sufficiently healthy condition (Fig. 7-I D). This area belongs to the southern part of the study region, which is known to be in the orographical "air pollution shadow" of the surrounding Polish and Czech Beskids (Šrámek, Sitková, Małek, Pavlenda, & Hlásny, 2010), where no significant emission sources were present. Besides the example area D, gradual increase in biomass was also observed in Wisła forest district in Poland, where local spruce provenance (Istebna spruce) occurs. It has been proven that natural Norway spruce populations under stress are genetically adaptable to local site conditions (Krajmerová & Longauer, 2000). Several local provenances (particularly Istebna provenance) achieve high growth and survival adaptations, while tolerating seasonal water shortcomings (Boratyński & Bugała, 1998; Longauer et al., 2010). We saw evidence of these acquired traits of spruce by the averaged gradual increase trajectory, established for the stable coniferous forest condition. This trajectory shows a linear increase of biomass from 156 Mg ha^{-1} in 1985 to 217 Mg ha^{-1} in 2010. The annual accumulation rates are constant throughout all considered years and reach 2.5 Mg ha^{-1} yr^{-1} (+/−0.04 Mg ha^{-1}) of biomass increase, beyond the first and the last considered year with ~2 Mg ha^{-1} and ~3 Mg ha^{-1}, respectively. These values are in line with the typical ranges reported for boreal and temperate coniferous forests dominated by spruce species (Boratyński & Bugała, 1998; McMahon et al., 2010). Although accumulation rates are stable across time, slight periodical fluctuations occurred. We found that these sudden periodical interruptions correlate significantly with the spring precipitation ($r = 0.62$). Additionally, the winter averaged air temperature (especially for February) seems to be significantly related to the accumulation rates ($r = 0.37$). Our findings are in accordance with general knowledge regarding spruce growth responses to climate variables (Boratyński & Bugała, 1998; Longauer et al., 2010). Nonetheless, the comprehensive interpretation of forest regeneration and gradual increase processes in relation to climate and climate changes is highly challenging, thus requiring further research.

Besides these outcomes that apply across the entire study area, the net biomass change map (Fig. 8) shows significant differences in biomass change patterns across countries. In Poland, biomass loss corresponds to broad openings with either linear or fuzzy patch borders (example areas A and C), while compact patches of small strip clear-cuts dominate in Slovakia (B and D). Yet, negative net change patterns dominated in both Poland and Slovakia. In contrast, the net biomass change map revealed an overall stable situation in the Czech part of the study area, beside a few small patches indicating biomass loss in the north-eastern part in Czech Republic. These findings confirm outcomes of a previous study (Main-Knorn et al., 2009) and underline differences in the forest management and the disturbance history between the Polish, Slovak and Czech part of the Beskids. Selective logging and local reforestation practices (individual seedlings of different species) along elevation gradients were typical for Poland, while clear-cuts followed by plantations were preferred in the Czech Republic and Slovakia (Main-Knorn et al., 2009). Accordingly, extensive spruce decline and related biomass loss occurred substantially earlier in the Czech Republic and Slovakia compared to Poland (early 1980s and mid-1990s, respectively), leaving a longer period for forest regeneration considering our monitoring period (Kozak, 1996; Kubikova, 1991).

5.1. Limitations and accuracy assessment

While our analyses yielded reliable biomass change maps with high temporal resolution, some sources of uncertainty remain. First, optical remote sensing has a limited sensitivity for reproducing biomass in dense forests, and is susceptible to the confounding effect of understory vegetation in sparse forests. Thus, as stated by for example Main-Knorn et al. (2011) or Blackard et al. (2008) a slight bias in biomass estimates may occur with tendency to over-predict lower and to under-predict higher biomass values. Additionally, due to data limitations, we only estimated live aboveground biomass, which disregards potential dead aboveground biomass allocated in snags and coarse woody debris. Second, although the LandTrendr fitting approach interpolates missing/masked pixel values and generally reduces phenology effects and inter-annual noise, uncertainties remain. For 1987 high omission error can be explained by a higher vulnerability of the fitting algorithm to outliers at the beginning of the time series. For 1994 and 2002, misclassifications are likely caused by high cloud coverage (17% and 13% of the total study area, respectively).

Third, the gradual increase class performs moderately in terms of omission and commission errors, and is confused with the no change class in case of misclassifications. This can be explained by low annual accumulation rates, particularly in old-growth forest stands, leading to confusion with the stable forest class.

Finally, no accuracy assessment of change magnitude was possible. In accordance with the regulations concerning forest protection procedures, bark beetle infested trees or stands should be removed within the same year through salvage logging, while wind-throw treatment depends on the timing, affected range, and potential insect pest risk (Instrukcja Ochrony Lasu, 2004). Hence, for wind-throw stands inventory data might still reflect previously standing tree volume, while our annual biomass estimates might register already the biomass loss.

6. Conclusions

In this study, we showed the effectiveness of the trajectory-based change detection approach (LandTrendr) to map abrupt and gradual biomass changes in the Western Carpathians. A near-annual time-series provided detailed information on stand-replacing disturbances, long-term degradation, and forest regeneration; processes that strongly affect forest biomass. The LandTrendr approach enabled us to spatially link estimates of forest biomass with disturbance and recovery information, which is crucial in order to understand the role of different disturbances on the carbon balance in the Carpathians. The main advantage of a near-annual time series approach over bi-temporal study on mapping disturbances is, that the first enables detecting long-term trends, while the latter could miss or under-estimate those.

Further, we demonstrated that imagery from SPOT-1 and IRS-LISS can be used to fill Landsat data gaps. The validation of the SPOT SWIR model showed highly significant results, making the incorporation of such a modified SPOT image into the Landsat time series feasible. We found no evidence that multi-sensor trajectory of Landsat, SPOT and IRS LISS data affected the standard deviation and the mean biomass estimation errors (Fig. 4). Similarly, the validation of the disturbance map revealed no discrepancies in accuracies when incorporating “Landsat-like” sensors (Table 2).

Putting our findings in a regional context, we found very complex disturbance history in the study area. Massive coniferous biomass loss between 1985 and 2010, triggered by the coincidental effect of biotic and abiotic drivers is evident. On the one hand, gradual disturbances were dominating in the study region, indicating increasing role of insects and pathogens in coniferous decline. On the other hand, abrupt disturbances intensified since 2005, revealing strong interactions between biomass loss and climate conditions. Total and net biomass change highlights negative biomass balance, suggesting, that the losses of the AGB were not balanced by the gains in our study area. To answer the question if coniferous forests in this area have converted from a net carbon sink to a net carbon source between 1985 and 2010, further data on biomass change in other carbon pools as for example wood products, dead biomass, belowground biomass, coarse woody debris, and soil organic carbon would be required (Houghton, 2005).

Despite the known limitations regarding the empirical modeling of biomass with optical remote sensing data, this study provides the first maps of biomass loss and accumulation rates in the spruce-dominated Western Carpathian forests. Advanced remote sensing approaches, such as the modeling of biomass and the application of trajectory-based change detection algorithms, provide spatially and temporally explicit quantifications of biomass variability within inventory stands. This study underlines that monitoring of spatio-temporal patterns of forest ecosystem dynamics is only feasible when applying enhanced remote sensing methods.

Acknowledgments

This study was supported by the Berlin Young Scientists Scholarship Fund (NaföG), Humboldt-Universität zu Berlin, US Forest Service Pacific NW Research Station in Corvallis, OR, USA, and the Belgian Science Policy (Stereo II, contract SR/00/133, FoMo project). We would like to thank ‘The State Forests National Forest Holding’, as well as J. Kozak and L. Kulla for their generous provision of data and photography. We are grateful to T. Kuemmerle and J. Knorn for providing insightful and constructive comments. Patrick Hostert gratefully acknowledges the support of the Landsat Science Team and the Global Land Project. Two anonymous reviewers contributed valuable comments.

References

Badea, O., Tanase, M., Georgeta, J., Anisoara, L., Peiov, A., Uhlirova, H., et al. (2004). Forest health status in the Carpathian Mountains over the period 1997–2001. *Environmental Pollution*, *130*, 93–98.

Barszcz, J., & Małek, S. (2008). Estimation of natural regeneration of spruce in areas under threat to forest stability at high altitudes of the Beskid Śląski Mts. *Beskydy*, *1*, 9–18.

Blackard, J. A., Finco, M. V., Helmer, E. H., Holden, G. R., Hoppus, M. L., Jacobs, D.M., et al. (2008). Mapping US forest biomass using nationwide forest inventory data and moderate resolution information. *Remote Sensing of Environment*, *112*, 1658–1677.

Boratyński, A., & Bugała, W. (1998). *Biologia świerka pospolitego*. Poznań: Wydawnictwo Naukowe Bogucki.

Breiman, L. (2001). Random forests. *Machine Learning*, *45*, 5–32.

Canty, M. J., Nielsen, A. A., & Schmidt, M. (2004). Automatic radiometric normalization of multitemporal satellite imagery. *Remote Sensing of Environment*, *91*, 441–451.

Capecki, Z. (1994). *Rejony zdrowotności lasów zachodniej części Karpat. (Health regions of the forests of the western Carpathian Mts)*. : Prace IBL, A, 61–125.

Card, D. H. (1982). Using known map category marginal frequencies to improve estimates of thematic map accuracy. *Photogrammetric Engineering and Remote Sensing*, *48*, 431–439.

Chavez, P.S. (1996). Image-based atmospheric corrections revisited and improved. *Photogrammetric Engineering and Remote Sensing*, *62*, 1025–1036.

Cochran, W. G. (1977). *Sampling techniques*. New York: NY: Wiley.

Cohen, W. B., & Goward, S. N. (2004). Landsat's role in ecological applications of remote sensing. *BioScience*, *54*, 535–545.

Cohen, W. B., Yang, Z. G., & Kennedy, R. (2010). Detecting trends in forest disturbance and recovery using yearly Landsat time series: 2 TimeSync — Tools for calibration and validation. *Remote Sensing of Environment*, *114*, 2911–2924.

Csóka, P. (2005). Capital management — The forests in countries in transition — Welfare impacts. In J. L. Innes, G. M. Hickey, & H. F. Hoen (Eds.), *Forestry and environmental change: Socioeconomic and political dimensions* (pp. 125–141). : CABI Publishing.

Cutler, D. R., Edwards, T. C., Beard, K. H., Cutler, A., Hess, K. T., Gibson, J., et al. (2007). Random forests for classification in ecology. *Ecology*, *88*, 2783–2792.

Davis, F., & Goetz, S. (1990). Modeling vegetation pattern using digital terrain data. *Landscape Ecology*, *4*, 69–80.

Ditmarová, L., Kmet', J., Ježík, M., & Vál̆ka, J. (2007). Mineral nutrition in relation to the Norway spruce forest decline in the region Horný Spiš (Northern Slovakia). *Journal of Forest Science*, *53*, 93–100.

Durło, G. (2010). The influence of pluvial conditions on spruce forest stands stability in Beskid Śląski Mts. *Acta Agrophysica, Meteorology and Climatology Research*, *2010*(5), 208–217.

Fitterer, J. L., Nelson, T. A., Coops, N. C., & Wulder, M.A. (2012). Modelling the ecosystem indicators of British Columbia using Earth observation data and terrain indices. *Ecological Indicators*, *20*, 151–162.

Frolking, S., Palace, M. W., Clark, D. B., Chambers, J. Q., Shugart, H. H., & Hurtt, G. C. (2009). Forest disturbance and recovery: A general review in the context of spaceborne remote sensing of impacts on aboveground biomass and canopy structure. *Journal of Geophysical Research — Biogeosciences*, *114*.

Goward, S., Arvidson, T., Williams, D., Faundeen, J., Irons, J., & Franks, S. (2006). Historical record of Landsat global coverage: Mission operations, NSLRSDA, and international cooperator stations. *Photogrammetric Engineering and Remote Sensing*, *72*, 1155–1169.

Griffiths, P., Kuemmerle, T., Kennedy, R. E., Abrudan, I. V., Knorn, J., & Hostert, P. (2012). Using annual time-series of Landsat images to assess the effects of forest restitution in post-socialist Romania. *Remote Sensing of Environment*, *118*, 199–214.

Grodzińska, K., & Szarek-Łukaszewska, G. (1997). Polish mountain forests: Past, present and future. *Environmental Pollution*, *98*, 369–374.

Grodzki, W. (2007). Spatio-temporal patterns of the Norway spruce decline in the Beskid Śląski and Żywiecki (Western Carpathians) in southern Poland. *Journal of Forest Science*, *53*, 38–44.

Grodzki, W. (2010). The decline of Norway spruce *Picea abies* (L.) Karst. stands in Beskid Śląski and Żywiecki: Theoretical concept and reality. *Beskydy*, *3*, 19–26.
Grodzki, W. (2012). Stan i prognoza występowania czynników szkodotwórczych w Beskidach (PL). In L. Z.K.Sitková (Ed.), Zvolen: Národné lesnícke centrum — Lesnícky výskumný ústav Zvolen.
Grodzki, W., McManus, M., Knizek, M., Meshkova, V., Mihalciuc, V., Novotny, J., et al. (2004). Occurrence of spruce bark beetles in forest stands at different levels of air pollution stress. *Environmental Pollution*, *130*, 73–83.
Hill, J., & Aifadopoulou, D. (1990). Comparative analysis of landsat-5 TM and SPOT HRV-1 data for use in multiple sensor approaches. *Remote Sensing of Environment*, *34*, 55–70.
Hlásny, T., Fabrika, M., Sedmák, R., Barcza, Z., Štěpánek, P., & Turčáni, M. (2010). Future of forests in the Beskids under climate change. In T. Hlásny, & Z. Sitková (Eds.), *Spruce forests decline in the Beskids* (pp. 157–173). Zvolen: National Forest Centre — Forest Research Institute Zvolen & Czech University of Life Sciences Prague & Forestry and Game Management Research Institute Jíloviště.
Hlásny, T., Grodzki, W., Šrámek, V., Holuša, J., Kulla, L., Sitková, Z., et al. (2010). Spruce forests decline in the Beskids. In T. Hlásny, & Z. Sitková (Eds.), *Spruce forests decline in the Beskids* (pp. 15–31). Zvolen: National Forest Centre — Forest Research Institute Zvolen & Czech University of Life Sciences Prague & Forestry and Game Management Research Institute Jíloviště.
Hlásny, T., Grodzki, W., Turčáni, M., Sitková, Z., & Konôpka, B. (2010). Bark beetle — The main driving force behind spruce forests decline. In T. Hlásny, & Z. Sitková (Eds.), *Spruce forests decline in the Beskids* (pp. 69–91). Zvolen: National Forest Centre — Forest Research Institute Zvolen & Czech University of Life Sciences Prague & Forestry and Game Management Research Institute Jíloviště.
Hlásny, T., & Sitková, Z. (2010). *Spruce forests decline in the Beskids*. Zvolen: National Forest Centre — Forest Research Institute Zvolen & Czech University of Life Sciences Prague & Forestry and Game Management Research Institute Jíloviště.
Houghton, R. A. (2005). Aboveground forest biomass and the global carbon balance. *Global Change Biology*, *11*, 945–958.
Huang, C., Goward, S. N., Masek, J. G., Thomas, N., Zhu, Z., & Vogelmann, J. E. (2010). An automated approach for reconstructing recent forest disturbance history using dense Landsat time series stacks. *Remote Sensing of Environment*, *114*, 183–198.
Instrukcja Ochrony Lasu [Instruction for Forest Protection] (2004). *Państwowe Gospodarstwo Leśne Lasy Państwowe*. Warszawa: Centrum Informacyjne Lasów Państwowych (276 pp.).
Kennedy, R. E., & Cohen, W. B. (2003). Automated designation of tie-points for image-to-image coregistration. *International Journal of Remote Sensing*, *24*, 3467–3490.
Kennedy, R. E., Cohen, W. B., & Schroeder, T. A. (2007). Trajectory-based change detection for automated characterization of forest disturbance dynamics. *Remote Sensing of Environment*, *110*, 370–386.
Kennedy, R. E., Yang, Z. G., & Cohen, W. B. (2010). Detecting trends in forest disturbance and recovery using yearly Landsat time series: 1 LandTrendr — Temporal segmentation algorithms. *Remote Sensing of Environment*, *114*, 2897–2910.
Kimball, J. S., Keyser, A.R., Running, S. W., & Saatchi, S. S. (2000). Regional assessment of boreal forest productivity using an ecological process model and remote sensing parameter maps. *Tree Physiology*, *20*, 761–775.
Knorn, J., Kuemmerle, T., Radeloff, V. C., Szabo, A., Mindrescu, M., Keeton, W. S., et al. (2012). Forest restitution and protected area effectiveness in post-socialist Romania. *Biological Conservation*, *146*, 204–212.
Kozak, J. (1996). Przestrzenny model degradacji lasów Beskidu Śląskiego. *Biuletyn KPZK*, *174*, 511–538.
Krajmerová, D., & Longauer, R. (2000). Genetická diverzita smreka obyčajného *Picea abies* Karst. na Slovensku [Genetic diversity of Norway spruce (Picea abies Karst.) in Slovakia]. *Forestry Journal*, *46*, 130–147.
Kubikova, J. (1991). Forest dieback in Czechoslovakia. *Vegetatio*, *93*, 101–108.
Kurz, W. A., Dymond, C. C., Stinson, G., Rampley, G. J., Neilson, E. T., Carroll, A. L., et al. (2008). Mountain pine beetle and forest carbon feedback to climate change. *Nature*, *452*, 987–990.
Kurz, W. A., Stinson, G., Rampley, G. J., Dymond, C. C., & Neilson, E. T. (2008). Risk of natural disturbances makes future contribution of Canada's forests to the global carbon cycle highly uncertain. *Proceedings of the National Academy of Sciences of the United States of America*, *105*, 1551–1555.
Lakida, P., Nilsson, S., & Shvidenko, A. (1996). Estimation of forest phytomass for selected countries of the former European USSR. *Biomass and Bioenergy*, *11*, 371–382.
Longauer, R., Gömöry, D., Pacalaj, M., & Krajmerová, D. (2010). Genetics aspects of stress tolerance and adaptability of Norway spruce. In T. Hlásny, & Z. Sitková (Eds.), *Spruce forests decline in the Beskids* (pp. 136–143). Zvolen: National Forest Centre — Forest Research Institute Zvolen & Czech University of Life Sciences Prague & Forestry and Game Management Research Institute Jíloviště.
Longauerová, V., Leontovyč, R., Krajmerová, D., Vakula, J., & Grodzki, W. (2010). Fungial pathogens — Hidden agents of decline. In T. Hlásny, & Z. Sitková (Eds.), *Spruce forests decline in the Beskids* (pp. 93–105). Zvolen: National Forest Centre — Forest Research Institute Zvolen & Czech University of Life Sciences Prague & Forestry and Game Management Research Institute Jíloviště.
Lu, D., Mausel, P., Brondizio, E., & Moran, E. (2004). Change detection techniques. *International Journal of Remote Sensing*, *25*, 2365–2407.
Luyssaert, S., Ciais, P., Piao, S. L., Schulze, E. D., Jung, M., Zaehle, S., et al. (2010). The European carbon balance. Part 3: Forests. *Global Change Biology*, *16*, 1429–1450.
Main-Knorn, M., Hostert, P., Kozak, J., & Kuemmerle, T. (2009). How pollution legacies and land use histories shape post-communist forest cover trends in the Western Carpathians. *Forest Ecology and Management*, *258*, 60–70.
Main-Knorn, M., Moisen, G. G., Healey, S. P., Keeton, W. S., Freeman, E. A., & Hostert, P. (2011). Evaluating the remote sensing and inventory-based estimation of biomass in the Western Carpathians. *Remote Sensing*, *3*, 1427–1446.
Materna, J. (1989). Air-pollution and forestry in Czechoslovakia. *Environmental Monitoring and Assessment*, *12*, 227–235.
Matiakowska, J., & Szabla, K. (2007). Beskidy bez lasu? *Magazyn Społeczno-Kulturalny "Śląsk"*. Katowice, Poland: Górnośląskie Towarzystwo Literackie.
McMahon, S. M., Parker, G. G., & Miller, D. R. (2010). Evidence for a recent increase in forest growth. *Proceedings of the National Academy of Sciences*, *107*, 3611–3615.
Meigs, G. W., Kennedy, R. E., & Cohen, W. B. (2011). A Landsat time series approach to characterize bark beetle and defoliator impacts on tree mortality and surface fuels in conifer forests. *Remote Sensing of Environment*, *115*, 3707–3718.
Mickler, R. A., Earnhardt, T. S., & Moore, J. A. (2002). Regional estimation of current and future forest biomass. *Environmental Pollution*, *116*, S7–S16.
Mijal, L., & Kulis, M. (2004). The threat to the spruce stands in the Ustron Forest District. *Forest Research Papers*, *1*, 140–143.
Moran, E. F., & Ostrom, E. (Eds.). (2005). *Seeing the forest and the trees. Human–environment interactions in forest ecosystems*. Cambridge, USA: MIT Press.
Muzika, R. M., Guyette, R. P., Zielonka, T., & Liebhold, A.M. (2004). The influence of O_3, NO_2 and SO_2 on growth of *Picea abies* and *Fagus sylvatica* in the Carpathian Mountains. *Environmental Pollution*, *130*, 65–71.
Pal, M., & Mather, P.M. (2005). Support vector machines for classification in remote sensing. *International Journal of Remote Sensing*, *26*, 1007–1011.
Pflugmacher, D., Cohen, W. B., & Kennedy, C. J. (2012). Using Landsat-derived disturbance history (1972–2010) to predict current forest structure. *Remote Sensing of Environment*, *122*, 146–165.
Pflugmacher, D., Cohen, W. B., Kennedy, R. E., & Yang, Z. (2013). Using Landsat-derived disturbance and recovery history and lidar to map forest biomass dynamics. *Remote Sensing of Environment* (in press).
Powell, S. L., Cohen, W. B., Healey, S. P., Kennedy, R. E., Moisen, G. G., Pierce, K. B., et al. (2010). Quantification of live aboveground forest biomass dynamics with Landsat time-series and field inventory data: A comparison of empirical modeling approaches. *Remote Sensing of Environment*, *114*, 1053–1068.
Powell, S. L., Pflugmacher, D., Kirschbaum, A. A., Kim, Y., & Cohen, W. B. (2007). Moderate resolution remote sensing alternatives: A review of Landsat-like sensors and their applications. *Journal of Applied Remote Sensing*, *1*, 1–15.
Prasad, A.M., Iverson, L. R., & Liaw, A. (2006). Newer classification and regression tree techniques: Bagging and random forests for ecological prediction. *Ecosystems*, *9*, 181–199.
Rull, V. (2011). Sustainability, capitalism and evolution — Nature conservation is not a matter of maintaining human development and welfare in a healthy environment. *EMBO Reports*, *12*, 103–106.
Schelhaas, M. J., Nabuurs, G. J., & Schuck, A. (2003). Natural disturbances in the European forests in the 19th and 20th centuries. *Global Change Biology*, *9*, 1620–1633.
Schroeder, T. A., Cohen, W. B., Song, C. H., Canty, M. J., & Yang, Z. Q. (2006). Radiometric correction of multi-temporal Landsat data for characterization of early successional forest patterns in western Oregon. *Remote Sensing of Environment*, *103*, 16–26.
Schroeder, T. A., Gray, A., Harmon, M. E., Wallin, D. O., & Cohen, W. B. (2008). Estimating live forest carbon dynamics with a Landsat-based curve-fitting approach. *Journal of Applied Remote Sensing*, *2*.
Schulp, C. J. E., Nabuurs, G. J., & Verburg, P. H. (2008). Future carbon sequestration in Europe — Effects of land use change. *Agriculture, Ecosystems and Environment*, *127*, 251–264.
Schulze, E. D. (1989). Air-pollution and forest decline in a spruce (*Picea abies*) forest. *Science*, *244*, 776–783.
Slodičák, M., Novák, J., Štefančík, I., & Kamenský, M. (2010). Silviculture measures and spruce stands conversion. In T. Hlásny, & Z. Sitková (Eds.), *Spruce forests decline in the Beskids* (pp. 145–155). Zvolen: National Forest Centre — Forest Research Institute Zvolen & Czech University of Life Sciences Prague & Forestry and Game Management Research Institute Jíloviště.
Šrámek, V., Sitková, Z., Małek, S., Pavlenda, P., & Hlásny, T. (2010). Air pollution and forest nutrition — What are their roles in spruce forest decline? In T. Hlásny, & Z. Sitková (Eds.), *Spruce forests decline in the Beskids* (pp. 49–67). Zvolen: National Forest Centre — Forest Research Institute Zvolen & Czech University of Life Sciences Prague & Forestry and Game Management Research Institute Jíloviště.
Šrámek, V., Vejpustková, M., Novotný, R., & Hellebrandová, K. (2008). Yellowing of Norway spruce stands in the Silesian Beskids — Damage extent and dynamics. *Journal of Forest Science*, *54*, 55–63.
Turnock, D. (2002). Ecoregion-based conservation in the Carpathians and the land-use implications. *Land Use Policy*, *19*, 47–63.
Wilson, E. H., & Sader, S. A. (2002). Detection of forest harvest type using multiple dates of Landsat TM imagery. *Remote Sensing of Environment*, *80*, 385–396.
Wulder, M.A., White, J. C., Coops, N. C., & Butson, C. R. (2008). Multi-temporal analysis of high spatial resolution imagery for disturbance monitoring. *Remote Sensing of Environment*, *112*, 2729–2740.